Apr 14th, 2022 - 2:00 PM

Scalar Susceptibility of a Diluted Classical XY Model

Reece Beattie-Hauser
Missouri University of Science and Technology

Scalar susceptibility of a diluted classical XY model

Reece Beattie-Hauser, Thomas Vojta
Missouri University of Science and Technology
April 4th, 2022

Abstract

The Higgs (amplitude) mode at the disordered superfluid-Mott glass quantum phase transition was recently shown to feature unusual localization properties that violate naive scaling [1,2,3]. To test whether analogous behavior also occurs in the classical case, we analyze the Higgs mode in a diluted 3D classical XY-model near the magnetic phase transition. We calculate the amplitude correlation function and the corresponding scalar susceptibility by means of Monte Carlo simulations. In contrast to the quantum case, we find that the scalar susceptibility fulfills naive scaling (employing the clean critical exponents, as expected from the Harris criterion) as the temperature is varied across the phase transition for several dilutions.

Introduction

Outside of applications, exciting new advances in the sciences do not usually make their way into the public sphere. Even what some might consider to be landmark discoveries are often overlooked by the general public. Obviously, there are exceptions to this. The discovery of the Higgs boson is one such exception. The Higgs boson is often said to be the particle that gives mass to matter, and while that is technically correct, the full explanation is much more complicated. Such an explanation is outside the scope of this paper, but a short explanation is necessary for the purpose of analogy. The Higgs boson, like all other elementary particles, is an excitation of its corresponding field, the Higgs field, which breaks a continuous symmetry. The Higgs boson has a parallel in materials, called the Higgs mode. Like the Higgs boson, the Higgs mode is a collective excitation in materials with broken continuous symmetry, but here it is in order parameter amplitude; specifically, it is an excitation of the order parameter amplitude.

The order parameter is a quantity that distinguishes two phases in matter, and depending on the phases one is interested in, what one refers to as the order parameter may vary. For example, if one were examining a ferromagnetic phase transition, then the order parameter would be the magnetization; for a ferroelectric transition, it would be the polarization; etc.. Here, it will be easiest to refer to a ferromagnetic transition, so the language for the remainder of this paper will reflect that. But it should be noted that our findings can still be applied to other phase transitions depending on what one defines the order parameter as.

A general decomposition for a continuous-symmetry order parameter is

$$\vec{\phi} = \phi_o (1+\rho)\hat{n} \tag{1}$$

where ϕ_o is the order parameter's average amplitude, ρ is the fluctuation in amplitude, and $\hat{n}$ is order parameter direction.

A useful tool for identifying the Higgs mode is the scalar susceptibility, which is the correlation function of ρ seen below:

$$\chi_{\rho\rho}(\vec{x}) = \langle \rho(\vec{x})\rho(0) \rangle \tag{2}$$

where $\vec{x}$ is a relative position, with the reference point taken to be the origin.

Previous research of the Higgs mode at the superfluid-Mott glass quantum phase transition [1,2,3] found that the Higgs mode follows the expected behavior in clean materials but

not in systems containing impurities or defects. The Higgs mode behaved like a well-defined particle with long lifetime all the way to the phase transition in clean systems, with its energy going to zero as expected. In specialist terms, the scalar susceptibility fulfilled naive scaling. However, in disordered systems, the Higgs mode loses its particle character at the phase transition, and instead has a short lifetime and a broad energy distribution. In specialist terms, the mode violated naive scaling.

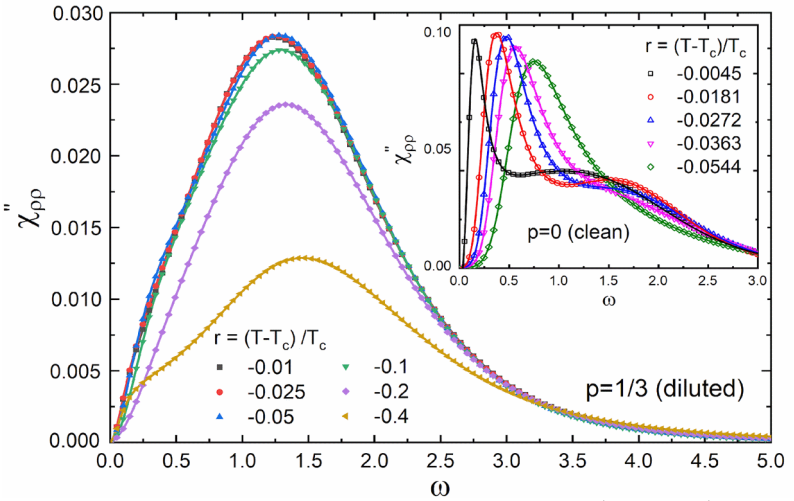

Figure 1. Scalar spectral function $\chi''_{\rho\rho}(\vec{q}=0\,,\,\omega)$. Main panel: dilution p=1/3. Inset: clean case (p=0). [1]

Figure 1 demonstrates the qualitative difference between the clean and diluted cases. In the clean case, the sharp peaks indicate a well-defined energy which softens (decreases to zero) as the system approaches the phase transition. This is contrasted by the diluted case, where the broader peaks imply a wider and not well-defined energy distribution which do not soften as the system approaches the phase transition.

These results are peculiar because the underlying thermodynamics of the system predict that the Higgs mode should fulfill naive scaling, yet the results clearly show that the Higgs mode violates naive scaling in the diluted system. This unexpected behavior merits further investigation. One particular question to be answered is if the Higgs mode behaves the same way in the classical case as it did in the quantum case or if it instead follows the expected behavior. We will be studying this question computationally by means of Monte Carlo.

Methods

To examine the behavior of the Higgs mode in a classical system, we will focus on a three-dimensional site-diluted XY model, according to the Hamiltonian

$$H=-J\sum_{\langle i\,,\,j\rangle}\varepsilon_i\varepsilon_j\vec{S}_i\cdot\vec{S}_j \tag{3}$$

which is a sum over pairs of nearest-neighbor sites on the cubic lattice, where *i* and *j* are indexes for sites on the lattice, with *j* being any of the sites adjacent to *i*. *J* is a constant related to the strength of interaction between sites on the lattice, $\vec{S}_i$ and $\vec{S}_j$ are two-dimensional unit vectors defined at each site (which are spin vectors for the ferromagnetic transition). Each ε is a random variable with:

$$\varepsilon = \begin{cases} 0 & \text{with probability } p \\ 1 & \text{with probability } 1-p \end{cases} \tag{4}$$

with p being the dilution concentration of a given system. Simply put, ε represents whether or not a particular lattice site is occupied by a magnetic atom or by a vacancy. There is a great number of configurations in which spin vectors and vacancies can be arranged for a given system size and dilution concentration, so it is necessary to simulate a representative sample of different configurations to ensure the statistical quality of our data.

To simulate the behavior of the Hamiltonian (3), we perform Monte Carlo simulations. Our simulation employs both the Wolff cluster [4] and Metropolis update [5] algorithms. The Wolff cluster algorithm updates spins for large clusters of sites simultaneously, helping to reduce the critical slowing-down caused by the Metropolis update algorithm, which updates spins individually. The Metropolis update algorithm is necessary, however, for updating isolated lattice sites that are not part of larger clusters. Each simulation sweep is a single Metropolis sweep followed by a Wolff sweep.

Each run of the simulation starts by initializing the system either at a "cold" start (ordered, with all spins initially parallel) or a "hot" start (disordered, with all spins random). The system is brought to thermal equilibrium by running 100 equilibration sweeps, during which no measurements are made, followed by 500 measurement sweeps. Results for hot and cold starts were compared to ensure that the system had reached thermal equilibrium.

The quantities calculated by the simulation that we are interested in are the scalar susceptibility (2), the Fourier transform of the scalar susceptibility (denoted $\widetilde{\chi}_{\rho\rho}$), and the Binder cumulant. The Binder cumulant is a dimensionless quantity defined as

$$g = 1 - \frac{\langle m^4 \rangle}{3\langle m^2 \rangle^2} \tag{5}$$

where m is the order parameter (magnetization), defined as

$$\vec{m} = \frac{1}{N} \sum_i \vec{S}_i \tag{6}$$

which is a sum of the spins of a site and its nearest neighbors. N is the number of spins being summed. Each site has six neighbors because our lattice is cubic, so $N = 7$.

The Binder cumulant will be used to determine the temperature where the phase transition occurs (called the critical temperature, T_c) and also to confirm the thermodynamic critical behavior of our clean and diluted systems.

The stability of a phase transition against disorder (impurities or defects) is famously governed by the Harris criterion [6]. It predicts that if $d \cdot \nu > 2$ (d being the dimensionality of the system and ν being the correlation length critical exponent), then the diluted system will exhibit thermodynamic critical behavior identical to that of the clean system. A high accuracy numeric value for ν has previously been calculated to be 0.6717 [8]. Thus, the Harris criterion is fulfilled, so our diluted systems are predicted to have the same thermodynamic critical behavior as our clean systems.

Plots of the Binder cumulant as a function of temperature share the same shape for a given impurity concentration, and furthermore, they intersect at the critical temperature. The calculation of T_c for each impurity concentration makes use of this characteristic by finding the temperature at which the Binder cumulants for different system sizes intersect with one another.

The point of intersection is weakly affected by finite-size effects, so it is important to not use systems sizes that are too small for this calculation.

The confirmation of the thermodynamic critical behavior makes use of finite-size scaling theory [7], according to which the Binder cumulant fulfills the scaling form

$$g(r, L) = Y(r L^{1/\nu}) \tag{7}$$

We start by taking the plots of the Binder cumulant as a function of distance from criticality r ($r = | T_c - T |$) and collapse them by rescaling the x-axis for each plot by a constant scale factor X such that all the plots overlap one another, forming a single curve. We then have a set of data points for the given dilution: one scale factor X for each linear system size L. These data points follow a power law of the form $X \sim L^{1/\nu}$, and a system's thermodynamic critical behavior is determined by the value of the exponent ν. Thus, if these data points for the clean and diluted systems follow the same power law, then they have identical thermodynamic critical behavior. The process of calculating the exponent ν for different dilutions involved finding the curve which best fit the data points, for which we used gnuplot's curve fitting function.

After our analysis of the Binder cumulant, we turned to the scalar susceptibility. An approximate functional form of the scalar susceptibility can be derived from scaling [1],

$$\chi_{\rho\rho}(r, x) \sim x^{2/\nu - 2d + 2} e^{-x/\xi} \tag{8}$$

Here, ξ denotes the correlation length, the range of the amplitude correlations. By fitting our data to this functional form, we computed values for the correlation lengths at different temperatures. The correlation length is expected to go to infinity at the critical temperature following the power law

$$\xi \sim r^{-\nu} \tag{9}$$

In the distance from criticality. Fitting the correlation lengthy data to this relation allows us to measure the exponent ν.

To determine if the Higgs mode fulfilled naive scaling, we examined the scalar susceptibility's scaling behavior. The scaling form for the scalar susceptibility (originally derived in [1]) for our model is

$$\widetilde{\chi}_{\rho\rho}(r, \vec{q}) = \widetilde{\chi}_o + b^{-d+2/\nu} \widetilde{\chi}_{\rho\rho}(r b^{1/\nu}, \vec{q} b) \tag{10}$$

where $\widetilde{\chi}_o$ is the noncritical contribution to the scalar susceptibility and b is an arbitrary scale factor. Setting $b = r^{-\nu}$ yields the form

$$\widetilde{\chi}_{\rho\rho}(r, \vec{q}) = \widetilde{\chi}_o + r^{d\nu - 2} X(\vec{q} r^{-\nu}) \tag{11}$$

where $X(\vec{q} r^{-\nu})$ is the scaling function of the scalar susceptibility.

We then computed the scale functions using our existing data for the scalar susceptibility and found each corresponding $\widetilde{\chi}_o$ according to the value which best collapses the scale functions. If the scale functions show a reasonable collapse, then the Higgs mode fulfills naive scaling.

Results

Over the course of our research, we tested several different dilution concentrations and system sizes. Table 1 shows all the dilution concentrations used along with their critical temperatures, as well as the effective values for the correlation length critical exponent ν obtained from the analysis of the Binder collapse, which will be discussed in greater depth shortly.

p	0 (clean case)	0.2	0.3	1/3	0.5
T_c	2.201844 [9]	1.671	1.39	1.2945	0.782
ν	0.6771	0.7150	0.7258	0.7306	0.7356

Table 1. List of critical temperatures for each dilution concentration tested. T_c for clean case found in [9].

The system sizes tested include L=24, 28, 32, 40, 50, 60, 70, 80, 100, and 128. All of the scalar susceptibility data is from systems with L=128, while the rest of the system sizes were used in the Binder cumulant analysis.

As previously discussed, the critical temperature for each dilution was computed by finding the point of intersection of the Binder cumulant. An example of such an intersection for $p = 0$ can be seen in the left panel of Figure 2.

The calculation of the scale factors for the Binder collapse was done numerically by finding the multiplier which best minimizes the area between two curves, using the largest system size (L = 100) as the "master" curve which all other curves were fit to. An example of the Binder collapse for $p = 0$ (using a small subset of systems) can be seen in the right panel of Figure 2.

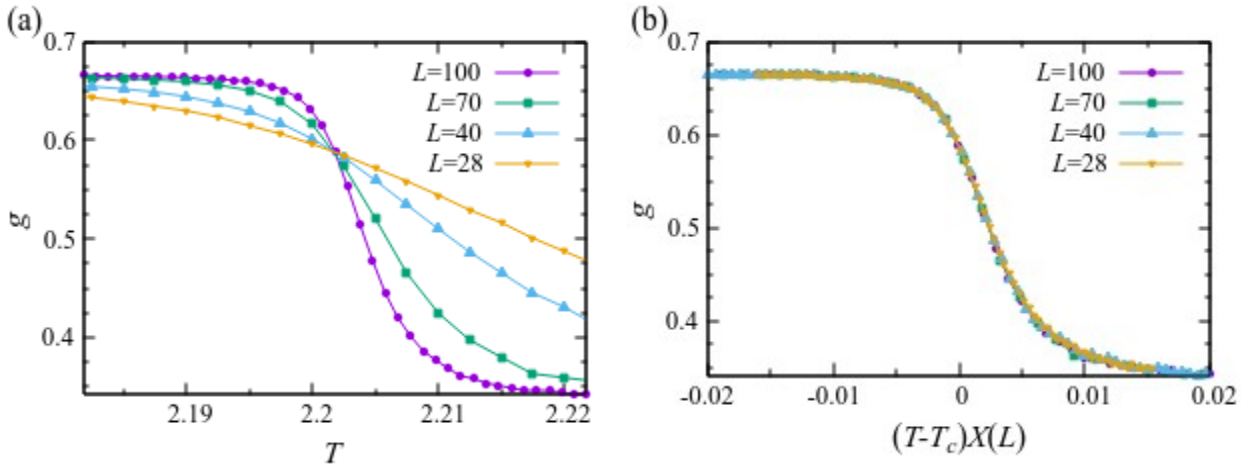

Figure 2. Binder cumulant for $p = 0$. (a) Plotted vs. absolute temperature, before collapse. (b) Plotted vs. rescaled distance from criticality, after collapse.

After obtaining the scale factors for the Binder collapse, we attempted to fit them to the functional form $X = a L^{1/\nu}$ with the expected value of $\nu = 0.6717$ and a being a fit parameter, but found that the resulting curve did not fit the data very well, only passing through the points at larger values of L. This is due to finite-size effects, and we will discuss this in more detail later. If we allow ν to be a fit parameter instead, the result is the plots seen in the left panel of Figure 3.

Since clean and diluted systems should be controlled by the same correlation length critical exponent, we added a multiplicative correction term of $(1+b L^{-\omega})$ to our functional form, where b and ω are fit parameters, and fixed ν to its expected value of 0.6717. The resulting fits can be seen in the right panel of Figure 3. As a side note, we found that ω was generally about 0.4 for different dilutions.

The quality of these fits demonstrates that both the clean and diluted systems are controlled by the same correlation length critical exponent, confirming their thermodynamic critical behavior to be identical as predicted by the Harris criterion.

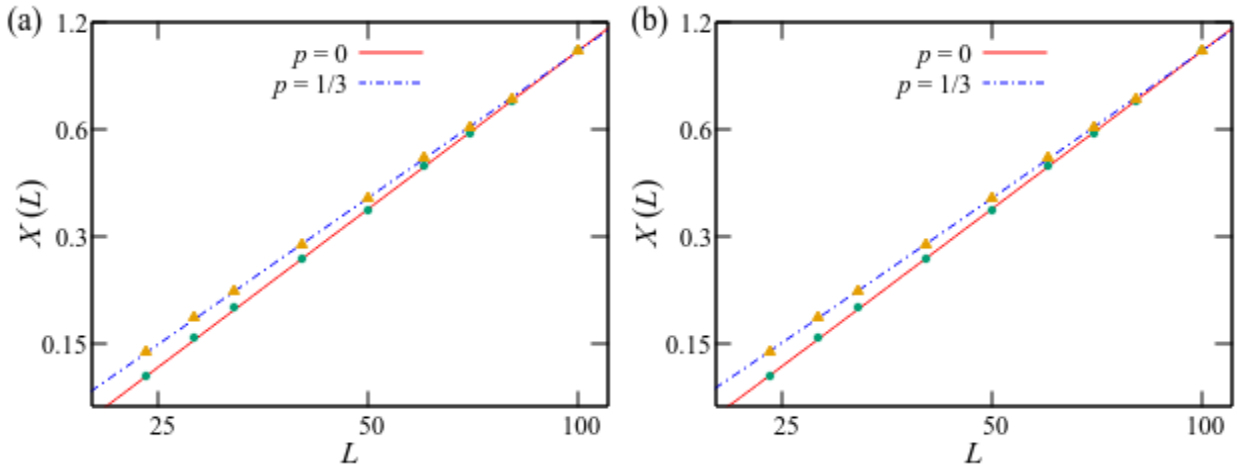

Figure 3. Fits of Binder collapse scale factors to functional forms, plotted on a log-log scale. (a) Fits to functional form $X = a L^{1/\nu}$ where a and ν are fit parameters, resulting in ν values found in Table 1. (b) Fits to functional form with correction term, $X = a L^{1/\nu}(1 + b L^{-\omega})$ where a, b, and ω are fit parameters but ν is fixed at the clean value 0.6717 [8].

Having confirmed the thermodynamic critical behavior of the clean and diluted systems, we continue to the focus of our research: the scalar susceptibility. Plots of the scalar susceptibility as a function of distance for the clean and diluted cases can be seen in Figure 4. The graphs shown are cut off where the data devolves into noise, which is the point where the scalar susceptibility dies out.

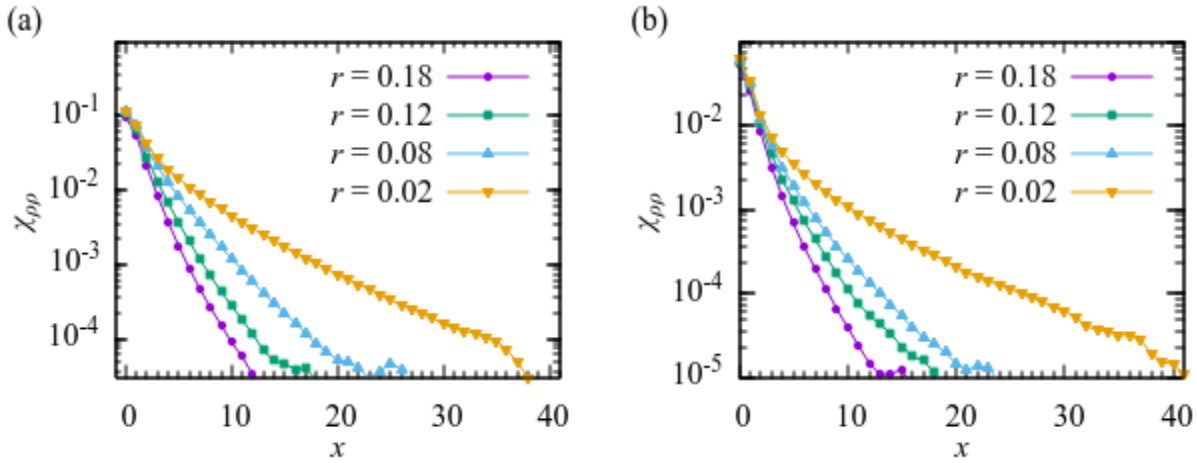

Figure 4. Scalar susceptibility as a function of distance on a semi-log scale. (a) clean case ($p = 0$). (b) diluted case ($p = 1/3$).

A cursory qualitative analysis of Figure 4 tells us that the scalar susceptibility survives to longer distances at temperatures closer to criticality, indicating longer correlation lengths. To

better calculate the correlation length, we fit our data to a functional form similar to (7), $\chi_{\rho\rho}=ax^{-1.02}e^{-x/\xi}$, where a and ξ are fit parameters. For these fits to succeed, it was vitally important to choose data ranges where the scalar susceptibility still survived. One example of such a fit can be seen in the main panel of Figure 5.

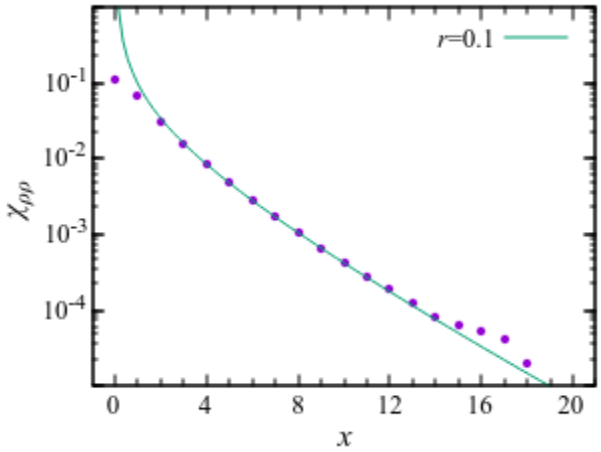

Figure 5. Example of a fit of the scalar susceptibility to functional form $\chi_{\rho\rho}=ax^{-1.02}e^{-x/\xi}$ for $r = 0.1$ ($T = 2.102$).

Once we obtained the correlation lengths for both the clean and diluted systems, we fit the data to the functional form $\xi=ar^{-\nu}$, where a and ν are fit parameters. We allowed ν to be a fit parameter instead of fixing it at its expected value to account for finite-size effects, the same reason as with the Binder collapse. These fits for the clean and diluted cases can be seen in Figure 6.

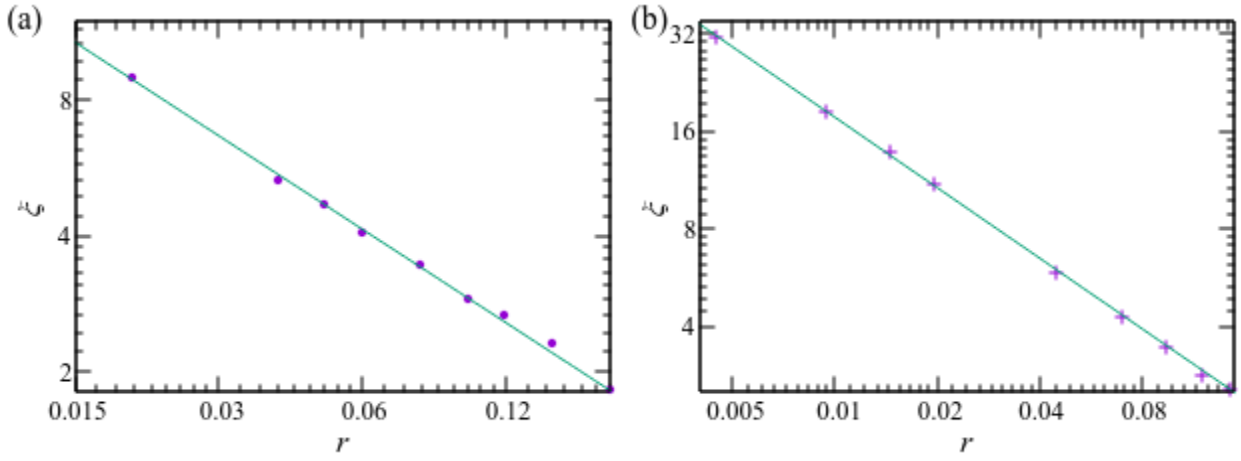

Figure 6. Fits of correlation lengths to functional form $\xi=ar^{-\nu}$ plotted on a log-log scale. (a) Clean case ($p = 0$); fit yielded $\nu = 0.69$. (b) Diluted case ($p = 1/3$); fit yielded $\nu = 0.72$.

While these fits are not as good as for the Binder collapse, they still demonstrate that both the clean and diluted systems exhibit the correlation length's expected behavior, meaning the correlation length goes to infinity at the critical temperature. It is also worth noting that the

values for ν that resulted from these fits are close to those found in the analysis of the Binder collapse.

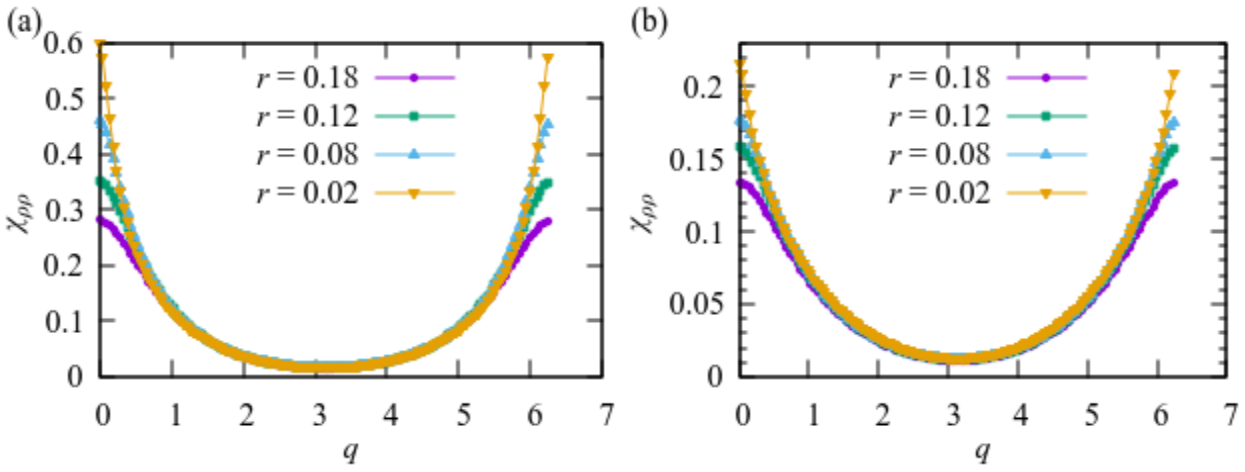

Figure 7. Fourier transform of scalar susceptibility as a function of wave number. (a) Clean case ($p = 0$). (b) Diluted case ($p = 1/3$).

To test the scaling behavior of the scalar susceptibility, we examined its Fourier transform. Plots of the Fourier transform of the scalar susceptibility can be found in Figure 7. Solving the scaling form (11) for the scaling function yielded

$$X(\vec{q}\, r^{-\nu}) = \frac{\widetilde{\chi}_{\rho\rho}(r, \vec{q}) - \widetilde{\chi}_o}{r^{d\nu - 2}} \tag{12}$$

Before we could compute the scaling function, we needed to pick a value for ν. As previously discussed, the correlation length critical exponent feels pronounced finite-size effects, so this is not as straightforward as it might seem. Using the expected value of $\nu = 0.6717$ resulted in scaling functions that collapsed reasonably well in the clean case, but collapsed very poorly in the diluted case. However, using the effective values for ν that we found in the analysis of the Binder collapse gave much better collapses. These scaling function collapses, both above and below the critical temperature, can be seen in Figure 8. While the collapses are not perfect by any means, they are of sufficient quality to say that naive scaling is fulfilled.

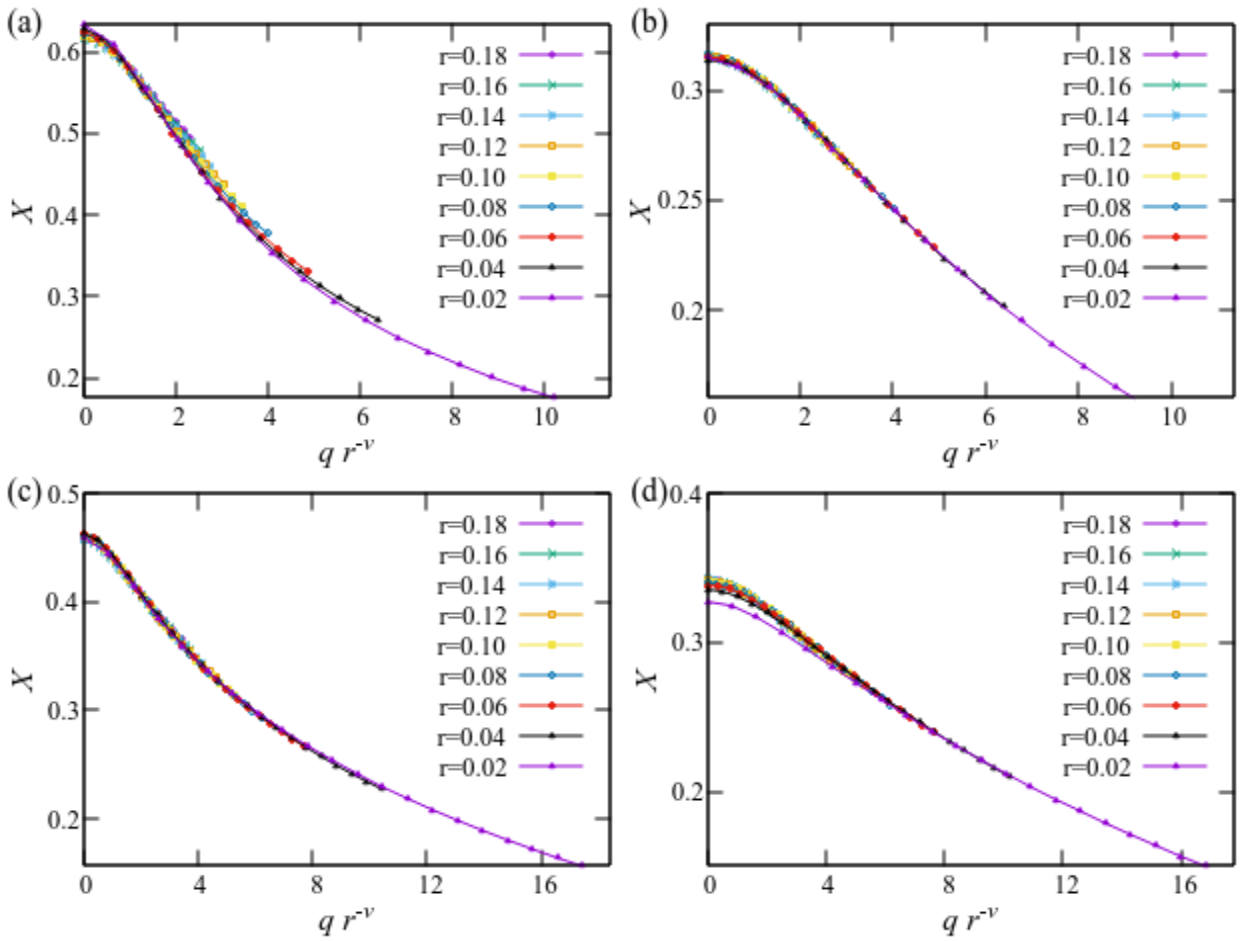

Figure 8. Plots demonstrating scale function collapses above and below the critical temperature.
(a) $p = 0$; below the critical temperature; used $\nu = 0.6771$.
(b) $p = 0$; above the critical temperature; used $\nu = 0.6771$.
(c) $p = 1/3$; below the critical temperature; used $\nu = 0.7306$.
(d) $p = 1/3$; above the critical temperature; used $\nu = 0.7306$.

Looking at the bottom-right panel of Figure 8, one can see quite clearly that the curve closest to criticality, $r = 0.02$, is significantly offset from the rest of the curves at the left-hand side of the graph. One possible explanation for this inaccuracy is that we could be lacking precision in our value for the critical temperature for $p = 1/3$. Since the scale function has a $1/r$ dependence, small inaccuracies in our value for the critical temperature will be more pronounced when r is close to zero. We do not see this in the clean case because its critical temperature is more precise, having seven significant digits, while our critical temperature in the $p = 1/3$ case is known only up to five significant digits.

Discussion

It would be remiss to not address all the corrections made to account for finite-size effects. Firstly, the expected value for the correlation length critical exponent, $\nu = 0.6717$, is the asymptotic value in the infinite system size limit. Getting closer to this expected value requires simulating larger and larger systems, which is problematic for a number of reasons. Most obvious is the increased computation time caused by large systems. Since we are simulating a

cubic system, the simulation time scales cubically with linear system size. Additionally, increasing the system size also increases the number of configurations we need to simulate, further extending the computation time. There is also the fact that the accuracy of our data increases logarithmically with linear system size, so increasing the system size has diminishing returns while also greatly increasing computation time. Combined, these factors impose a serious limitation on the kind of data we can collect within a reasonable time frame.

With these limitations in mind, it is clear that some accommodations are necessary, hence the "effective" values for the correlation length critical exponent found in Table 1. It is also of interest that the same values found through the analysis of the Binder collapse appear to describe the scale function collapse as well, and perhaps even the fits of the correlation lengths, though that is not something that we tested thoroughly.

In conclusion, we found that the Higgs mode in both clean and diluted systems in the classical case have the same critical behavior and agree with naive scaling. This contrasts what was previously found in the quantum case, where the diluted system exhibited unexpected behavior, differing from the clean system, and violated naive scaling. This will stimulate further research and advance our understanding of phase transitions in disordered systems.

Acknowledgments

I would like to give special thanks to Dr. Thomas Vojta for his guidance and patience. He is also responsible for the Pegasus IV computing cluster which the simulations were run on. Needless to say, none of this would have been possible without him.

This work was supported in part by the National Science Foundation under Grants No. DMR-1828489 and No. OAC-1919789.

References

[1] M. Puschmann, J. Crewse, J. A. Hoyos, and T. Vojta, Phys. Rev. Lett. **125**, 027002 (2020).
[2] J. Crewse and T. Vojta, Phys. Rev. B **104**, 014511 (2021).
[3] M. Puschmann, J.C. Getelina, J.A. Hoyos, and T. Vojta, Ann. Phys. **435**, 168526 (2021)
[4] U. Wolff, Phys. Rev. Lett. **62**, 361 (1989).
[5] N. Metropolis, A. Rosenbluth, M. Rosenbluth, E. Teller, and A. Teller, J. Chem. Phys. **21**, 1087 (1953).
[6] A. B. Harris, J. Phys. C **7**, 1671 (1974).
[7] M. N. Barber, in *Phase Transitions and Critical Phenomena*, edited by C. Domb and J. L. Lebowitz, Academic, New York, Vol. 8, p. 145. (1983)
[8] M. Campostrini, M. Hasenbusch, A. Pelissetto, and E. Vicari, Phys. Rev. B **74**, 144506 (2006).
[9] T. Vojta, J. Crewse, M. Puschmann, D. Arovas, and Y. Kiselev, Phys. Rev. B **94**, 134501 (2016).